

INTERNATIONAL SOCIETY FOR SOIL MECHANICS AND GEOTECHNICAL ENGINEERING



This paper was downloaded from the Online Library of the International Society for Soil Mechanics and Geotechnical Engineering (ISSMGE). The library is available here:

<https://www.issmge.org/publications/online-library>

This is an open-access database that archives thousands of papers published under the Auspices of the ISSMGE and maintained by the Innovation and Development Committee of ISSMGE.

The paper was published in the proceedings of the 11th International Conference on Scour and Erosion and was edited by Thor Ugelvig Petersen and Shinji Sassa. The conference was held in Copenhagen, Denmark from September 17th to September 21st 2023.

Severe seabed response around marine structures: Numerical modelling of seabed liquefaction

C. Windt^{1,*}, V.S.O. Kirca², B.M. Sumer², S. Schimmels³, M. Kudella³, H. Rusche⁴, R. Shanmugasundaram⁴, V. Vanjakula⁵, F. Adam⁵, D. Majewski⁶, K. Kazimierowicz-Frankowska⁶, M. Pietrzekiewicz⁷, N. Goseberg^{1,3}

¹Technische Universität Braunschweig, Leichtweiß-Institute for Hydraulic Engineering and Water Resources, Braunschweig, Germany; *Email: c.windt@tu-braunschweig.de

²BMSUMER Consultancy & Research, Istanbul, Turkey

³Coastal Research Centre, Hannover, Germany

⁴WIKKI GmbH, Wernigerode, Germany

⁵GICON GmbH, Rostock, Germany

⁶Institute of Hydro-Engineering of the Polish Academy of Sciences, Gdansk, Poland

⁷PROJMORS Designing Office for Maritime Structures Co. Ltd., Gdansk, Poland

ABSTRACT

Recently, an ever-growing use of the ocean, e.g. for energy production, can be observed. The design of novel marine technologies renders challenging due to high demands on (cost-) efficiency and sustainability. Among the design aspects, understanding of the seabed response around marine structures is essential. The project "Numerical modelling of liquefaction around marine structures" develops a modelling framework for liquefaction around marine structures, including implementation, calibration, and validation. This paper presents the modelling framework, implemented in the OpenFOAM[®] CFD toolbox, and shows some initial numerical results. Furthermore, the calibration and validation strategy based on small and large scale experiments, respectively, is detailed. It is shown that the use of the drift flux model together with an extension of the Biot consolidation equations enables the modelling of the entire liquefaction process. Furthermore, the potential for a future integrated liquefaction and scour model is briefly discussed.

INTRODUCTION

Supporting the mitigation of anthropogenic climate change by a transition towards a carbon free energy supply is one of the pressing challenges for humankind. The increased exploitation of wind energy, particularly offshore, can be seen as one of the main contributors to this transition. While fixed offshore wind installations are operating on a commercial scale already, floating offshore wind did not reach the same level of maturity yet. However, the abundant higher wind speeds and, thus, the larger exploitable capacity render floating offshore wind commercially appealing despite the additional design challenges.

Compared to their bottom fixed counterpart (monopole, jackets, etc.), floating offshore wind turbines (FOWT) face design challenges with respect to the anchoring (drag embedment anchors, suction buckets, gravity anchors), similar to those from classical offshore engineering examples (e.g. oil & gas rigs). However, a direct mapping of classical offshore designs to FOWT is prevented by the significantly tighter restraints on cost efficiency for offshore wind installations.

The seabed response (scour and liquefaction) around marine structure, and anchoring components in particular, is one aspect of the anchoring design challenges for FOWT. Recently, Sumer and Kirca (2021) reviewed scour and liquefaction issues for anchors and other subsea structures in floating offshore wind farms and conclude that these issues are largely overlooked for such types of marine structures. The authors present numerical examples for the scour around a tensioner and the wave-induced liquefaction around a drag embedment anchor (DEA). While the authors show significant sinking depths for the DEA when liquefaction is triggered, the authors remark that the pressure (in excess of the static pressure) at large water depths does not penetrate down to the seabed. Thus, the wave-induced cyclic shear stresses/strains and, thus, liquefaction may not be triggered. This statement may be reviewed, in particular for severe sea states and for other types of anchoring systems. In particular, tension leg platform (TLP)-type FOWTs with gravity anchors transfer wave-induced loads on the floating structure down to the gravity anchor and, hence, the seabed, leading to wave and structural loading, showing a potential to trigger liquefaction.

Being able to predict and assess the (potential for) liquefaction around marine structures, such as gravity anchors, under combined wave and structural loading is therefore crucial in order to design cost-efficient and durable FOWTs. The acquired knowledge can support, for instance, the shape optimization of gravity anchors, the design and evaluation of scour protection systems, and the site selection for offshore wind installations.

To date, the prediction and assessment of liquefaction around marine structures relies on numerical and experimental modelling approaches. However, limitations, such as the negligence of the change of state of solid soil or the influence of model uncertainties, can be identified for either of these modelling approaches in order to allow an efficient and comprehensive analysis of liquefaction for engineering design purposes, including pore-pressure build up, modelling of liquefied soil, and compaction (Windt, et al., 2022).

Objectives: To overcome these limitations, the project “Numerical modelling of seabed liquefaction around marine structures” (NuLIMAS, 2020) aims to develop a holistic, OpenFOAM-based, numerical model for seabed liquefaction, following the sequential steps of (i) Numerical implementation; (ii) Model calibration; (iii) Model validation. Dedicated experimental test campaigns at small and large scale will be conducted for the model calibration and validation, respectively. In particular, for the model validation, the GICON TLP-type FOWT is employed as case study. This paper presents an overview of the NuLIMAS projects and

- Provides details of the numerical implementation and experimental test campaigns.
- Shows initial numerical results
- Identifies the pertinent future work towards the extension of the model for the modelling of scour and erosion processes.

The remainder of the paper is structured as follows. Section 2 will give a brief overview of the general mathematical modelling approach for seabed liquefaction. Furthermore, the section features a brief elaboration on the implications of liquefaction on scour around marine structures. Following on, Section 3 presents the numerical implementation of the hydro-geotechnical processes for seabed liquefaction (pore pressure build-up, state of change solid-liquid, state of change liquid-solid), including some initial results. Section 4 then details the calibration and validation strategy. Finally, in Section 5, conclusions are drawn and future work is suggested.

SEABED LIQUEFACTION

Seabed soil can lose its bearing capacity when pore pressure accumulates. Cyclic shear stress induced, for instance, by seismic loading or cyclic surface wave action, can trigger such an accumulation: In undrained conditions loosely packed soil grains under shear stress show a tendency to rearrange and contract, resulting in a decrease of pore volume in-between the grains. The decrease of the pore volume leads to an increase in pore pressure and, in turn, a tendency of the pore water to flow out of the pore volume. However, in undrained conditions, the flow out of the pore volume is not permitted and pore pressure accumulates. Following Terzaghi's principle, the increased pore pressure results in a reduction of the normal effective stress in the soil volume up to a point where the soil effectively loses its bearing capacity, changing its state from solid to liquid (i.e. liquefaction). After liquefaction, a pore pressure gradient triggers the settling of soil grains, resulting in the change of state from liquid to solid soil (i.e. compaction).

Modelling of seabed liquefaction: Considering the seabed soil as poro-elastic solid, Biot's theory on poro-elasticity (Biot, 1941) forms the basis for models of seabed liquefaction. Two equations are derived for the linear momentum balance and the pore fluid continuity:

$$G\nabla^2 U + \frac{G}{1-2\nu}\nabla\varepsilon = \nabla p \quad (1)$$

$$\frac{k}{\gamma}\nabla^2 p = \frac{n}{K'}\frac{\partial p}{\partial t} + \frac{\partial\varepsilon}{\partial t} \quad (2)$$

In Eq. (1) and (2) G denotes the shear modulus, ν the Poisson ratio, U the displacement vector, ε is the volumetric strain, and p is the phase-resolved pore fluid pressure. k denotes the hydraulic conductivity and γ denotes the specific weight of the soil n is the porosity, and K' is the true bulk

modulus of elasticity of water (Verruijt, 1969). For a more detailed derivation, the interested reader is referred to (Shanmugasundaram, et al., 2022).

Eqs. (1) and (2) do not cater for the build-up of the pore pressure. To that end, Sumer (2014) provides a description for the pore pressure build-up:

$$\frac{\partial P}{\partial t} = c_v \frac{\partial^2 P}{\partial z^2} + \frac{\sigma_0'}{N_l T}, \quad \text{with } N_l = \left(\frac{1}{\alpha_N} \frac{A_\tau}{\sigma_0'} \right)^{\frac{1}{\beta}} \quad (3)$$

where P is the accumulated pore pressure, c_v is the coefficient of consolidation. The last term in Eq. (3) represents a source term to account for the accumulation of pore pressure. In this source term, σ_0' is the initial mean normal effective stress, T is the wave period, and N_l the required number of cycles for liquefaction to set in. α_N and β are empirical constants (De Alba et al., 1976) and A_τ is the amplitude of the shear stress.

Following Sumer (2014), in this paper, residual liquefaction is defined to set in when the accumulated pore pressure is larger than σ_0' . Until soil liquefaction, the soil behaves like a poro-elastic solid. In contrast, the liquefied soil behaves like a highly viscous fluid and the whole constitutive relation changes. The liquefied soil is a two-phase flow with soil particles and water. This multiphase phase problem is approached using a drift flux model in which continuity equations and the momentum equations of the individual phases can be added. This addition gives one continuity equation and one momentum equation for the whole mixture so that the numerical instabilities from the momentum transfer can be eliminated. However, an additional equation needs to be solved for the drift flux. The governing equations of the liquefied soil are

$$\frac{\partial \rho}{\partial t} + \nabla \cdot \rho V = 0, \quad (4)$$

$$\frac{\partial \rho V}{\partial t} + \nabla \cdot \rho V V = -\nabla p + \rho g - \nabla \cdot \left(\frac{\alpha}{1-\alpha} \frac{\rho_c \rho_d}{\rho} V_{dj} \cdot V_{dj} \right), \quad (5)$$

$$\frac{\partial \rho \alpha}{\partial t} + \nabla \cdot \rho V \alpha = -\nabla \cdot \rho V_{dj} \alpha, \quad (6)$$

where α is the void fraction of soil grains. ρ_c , ρ_d , ρ are the densities of continuous phase, discrete phase, and mixture, respectively. V_{dj} is the drift velocity according to (Sumer, 2014).

As the pore pressure builds up, an upward-directed pressure gradient is generated, such that the accumulated pressure is largest at the impermeable base and smallest at the mudline, hence generating an upward-directed pressure gradient. This pressure gradient drives the water in the liquefied soil upwards, while the soil grains settle through the water until they begin to get into contact with each other. This process is known as soil compaction. The behavior of the bed

changes from essentially liquid in the upper layer to essentially solid (soil is denser) in the lower layer. There will be no change in pore pressure buildup after liquefaction until compaction occurs.

Implications on scour: Sumer and Kirca (2021), in their review of scour and liquefaction issues for anchors and other subsea structures state that the concept of scour breaks down once seabed soil changes its state from solid to liquid. However, the triggering factor of seabed liquefaction, i.e. pore pressure accumulation, can lead to a weakening of the seabed and, thus, increase the susceptibility to scour. Tonkin et al. (2003) investigate the tsunami-induced scour around a cylinder and find that the building up of a pore pressure gradient can significantly increase the scour rate. In their experiments, the authors observe such rapid scour for pore pressure gradients of “about one-half of that required for [momentary] liquefaction”. A similar observation is documented in (Sumer, 2014). However, to date, systematic analysis of the potential of soil weakening due to pore pressure build up is missing (Sumer and Kirca, 2021).

Once liquefied and compacted, higher density of the sand prevails, compared to pre-liquefaction soil density. Sumer et al. (2007) investigate the wave-induced scour around a pile for medium dense (pre-liquefaction) and dense (post-liquefaction) sand. The authors reveal a correlation between the soil density and the scour depth, which they explain via the increase of the friction angle.

NUMERICAL IMPLEMENTATION

The existing literature on the numerical modelling of seabed liquefaction reveals, a few numerical models for the analysis of seabed dynamics and liquefaction (Windt, et al., 2023). However, for the entire (residual) liquefaction and compaction process (pressure build-up, state of change from solid to liquid and back), no comprehensive model is currently available, including pore. This lack motivates the development, calibration, and validation of a numerical model for the liquefaction around marine structures in the OpenFOAM® framework.

In particular, the governing equations (1) – (6) are implemented in order to model the complete liquefaction sequence in a domain as depicted in Figure 1. Here, three main modelling areas are defined. To include the progressing gravity waves, Ω_1 represents the time varying pressure boundary conditions, with pressure magnitudes from linear wave theory. For the soil, Ω_2 and Ω_3 represent the regions of solid and liquefied soil, respectively. Ω_2 is governed by the Biot consolidation equations and the pore pressure build-up, while the drift flux model govern Ω_3 .

Initial results: A case study from Sumer et al. (2012) is considered to perform a first test of the implementation of the change of state from solid to liquid soil. The soil and wave properties are listed in Table 1. A simple rectangular box is generated to represent the soil region. The length of the considered domain is equal to one wave length and the height is equal to soil depth h .

Figure 2 (a) shows the progress of liquefaction front under the action of waves. By applying Biot consolidation equations and the pressure build-up equation, the liquefaction sets in after 7

seconds. The results show that the liquefaction begins from the mudline and progress downwards, thereby following the results provided by Sumer et al. (2012).

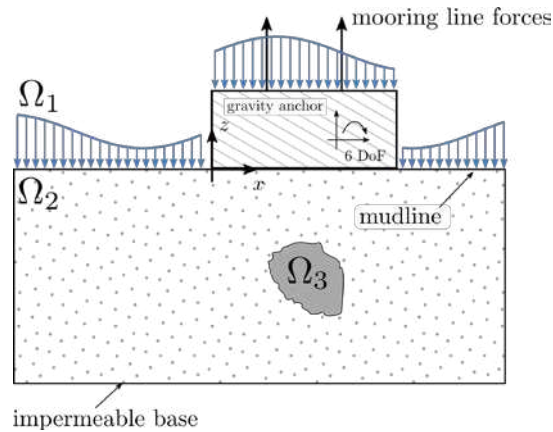


Figure 1: Schematic of the numerical setup. Ω_1 represents the pressure boundary conditions stemming from linear wave theory. Ω_2 and Ω_3 represent the regions of solid and liquefied soil, respectively. (Figure adapted from (Shanmugasundaram, et al., 2022)).

The same case study is considered to test the implementation for the change of state from liquid to solid soil. To that end, the simulation is restarted after 9.5 seconds with the wave pressure boundary being switched off. The liquefied soil is then allowed to settle without the waves.

Figure 2 (b) shows the progress void ratio of soil grains α at four different time instances. The results show that, as the soil settles, the water molecules moves upwards due to the upward directed pressure gradient. Contrary, the soil settles down at the bottom, increasing the volume fraction of soil grains. This matches with the experimental observations in (Sumer et al., 2012), as the compaction front progress upwards from the impermeable base to the mudline.

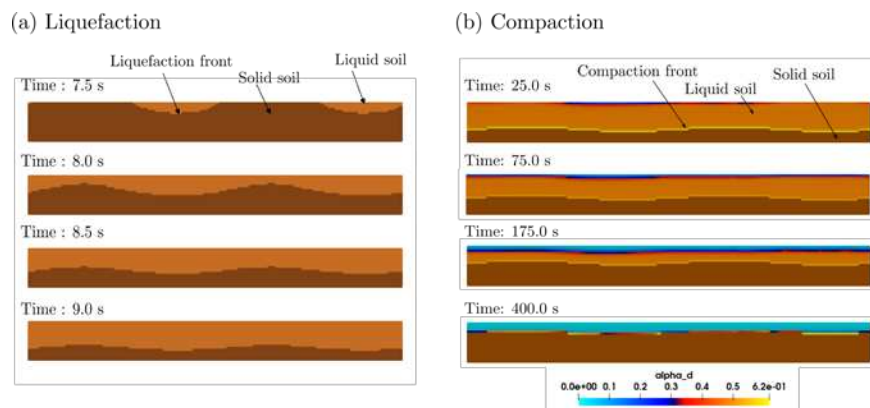


Figure 2: Example results of (a) the propagation of the liquefaction front. The color code serves as indicator: Dark brown is solid soil and light brown is liquefied soil; (b) the compaction of the liquefied soil after waves are stopped to propagate. The color code here refers to the void fraction of soil grains

Table 1. Physical properties of the wave and seabed

Physical Property	Value	Unit
Soil depth h	0.4	m
Poisson ratio μ	0.29	-
Porosity n	0.51	-
Permeability k	1.5×10^{-5}	m/s
Elastic modulus E	5	MPa
Degree of saturation S_r	1	-
Empirical constants [$\alpha_N \beta$]	[0.174 -0.36]	-
Wave height H	0.18	m
Wave period T	1.6	s
Water depth d	0.55	m
Porosity of compacted soil n_c	0.354	-

CALIBRATION & VALIDATION

Small scale experiments: For the calibration, reference data for seabed liquefaction on a process level are required, such that the required modelling coefficients (e.g. elastic moduli, Poisson's ratio, and coefficient of permeability) can be adjusted and basic model assumptions can be verified. To that end, small scale wave flume experiments have been conducted (see Figure 3).

Four different test cases, of varying complexity have been considered: (i) Waves-only; (ii) Wave-anchor-soil interaction; (iii) anchor-soil interaction; (iv) anchor settlement. For (i) and (ii) 19 different wave conditions with varying wave heights and periods have been tested, while the pore-pressure is measured at four specific locations in the soil pit.

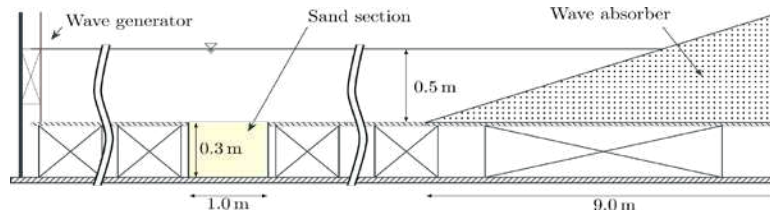


Figure 3: Experimental wave flume at IBW-PAN used for the small scale experiments.

Initial results: Examples results of the pore pressure along the soil column at four different depths ($Z=10, 15, 20, 25$ cm) are shown in Figure 4 for four different wave heights ($H=0.05, 0.10, 0.15, 0.20$ m) with a wave period of $T=1.3$ s. Figure 4 includes experimental (dashed lines), as well as numerical results (solid lines). It should be noted that the numerical results stem from the model for the onset of liquefaction and are, thus, only valid until liquefaction occurs, i.e. $P > \sigma_0'$, which is indicated by the dashed black line. In Figure 4, it can be observed that all wave heights but $H=0.05$ m trigger liquefaction in the soil pit in the physical tests. While for $H=0.20$ and 0.15 m similar trajectories of the pore pressure with steep gradients in the initial build-up phase can be observed, the pore pressure time trace for $H=0.10$ m shows slight differences in comparison. More detailed analysis of the pore pressure is published in (Kazimierowicz-Frankowska et al., 2022) and (Kazimierowicz-Frankowska et al., 2023). Comparing the numerical with the experimental results,

similarities and some differences can be observed. For the smallest wave height ($H=0.05$ m) good agreement between the numerical and experimental pore pressure trace can be observed. For $H=0.20$ m and $H=0.15$ m, liquefaction is triggered in the numerical model shortly after the start of the simulation. It should be noted that, different than for the experimental tests, no ramping of the wave action is implemented, leading to immediate pore pressure build-up, thereby explaining the slight differences between the experimental and numerical results. Clear differences between the numerical and experimental data can be observed for $H=0.10$ m. Further analysis is required to identify the source of this deviation.

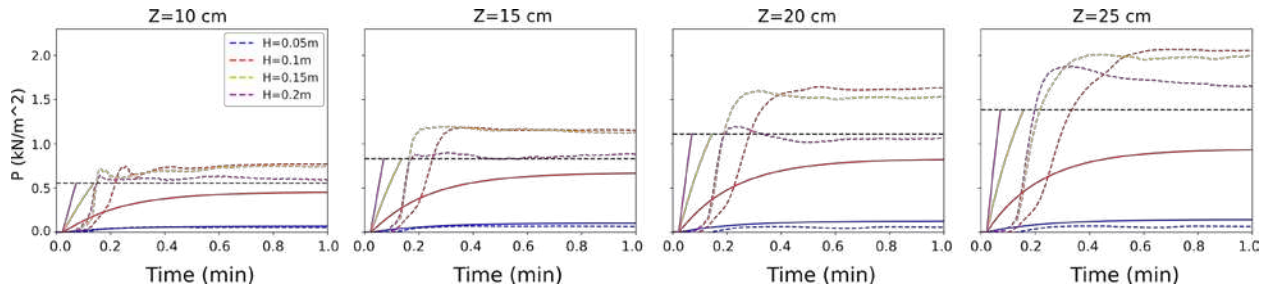


Figure 4: Initial results of the pore pressure from experimental tests (dashed lines) and numerical simulation (solid lines) for different wave heights with $T=1.3$ s. Pore pressure is measured along the soil column at four different depths. The black dashed line indicates σ_0' .

Large scale experiments: For the model validation, a realistic, large scale (i.e. 1/15) test case of a FOWT is considered. The experimental test campaign will be conducted in the *Large Wave Flume+* (GWK+) at the Coastal Research Center, a joint research facility of Leibniz University Hannover and Technische Universität Braunschweig, Germany. With dimensions of (length x width x depth) 307 m x 5m x 7 m and an installed wave maker capable of generating (extreme) wave heights of up to 3 m and periods up to 10 s, GWK+ allows testing of severe environmental loading at large scale. To enable testing of seabed dynamics and realistic offshore foundations, a deep pit of 1 m depth and 6 m length is used within the NuLIMAS project. For the large scale experiments, 16 pore pressure transducers are installed along the seabed (see Figure 5). Furthermore, anchor displacement is measured using echo sounders and mooring line loads are recorded using load cells.

As for the small scale experiments, two cases of incrementally increasing complexity are considered at large scale. First, cases featuring only wave excitation on the seabed are conducted, serving to acquired data for a scale comparison and, furthermore, to determine the optimal test conditions for the more complex test including the offshore wind turbine. For the setup including the offshore wind turbine, the foundation is placed on the seabed and the floating structure is connected to the foundation via four mooring lines.

For the realistic loading on the structure, wind loads are considered in addition to the wave excitation. To that end, a novel large scale multi-fan hardware-in-the-loop (HIL) system is developed. Wind loads are determined in real time based on the provided input wind field and the

displacement data of the floating structure, measure during the experiments using a Qualisys motion tracking system. A simplified low-order numerical model, initially developed by Lemmer (2018), is then employed to calculate the required load on the floating structure. In order to meet real-time requirements, the numerical model is reduced to only include the aerodynamics via a quasi-static actuator disk model; tower and/or blade dynamics are neglected.

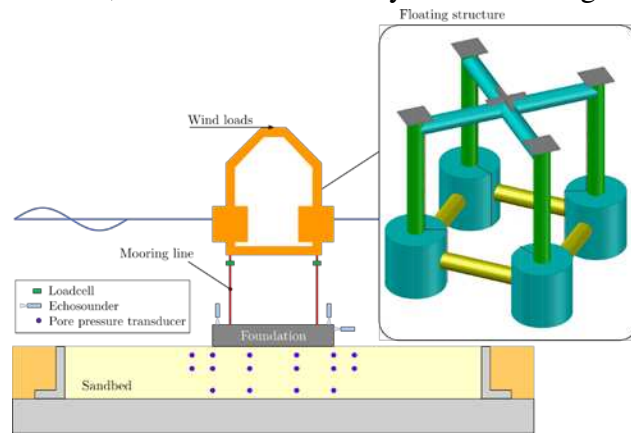


Figure 5: Schematic depiction of the large scale experimental test setup including an isometric view of the floating structure.

CONCLUSION & FUTURE WORK

This paper provides an overview of the development, calibration, and validation of a numerical model for the liquefaction around marine structures in the framework of the NuLIMAS project. The following conclusions can be drawn:

- Using the drift flux model together with an extension of the Biot consolidation equations enables the modelling of the entire liquefaction process, including pore pressure build-up and change of state of the soil.
- Dedicated experiments are required for model calibration and validation; however, require significant effort for preparation and execution in order to acquire meaningful results.

Future work: As discussed by Sumer and Kirca (2021) and highlighted in Section 2, systematic investigation of the implications of pore pressure build-up for the weakening of seabed soil, and, thus, its susceptibility to scour is largely under-explored. Given the complexity of the required model setup in physical test campaigns, numerical model can provide detailed insights. However, to that end, numerical modelling capabilities need to be developed. In future work, a “holistic” numerical model is needed, which is able to include both liquefaction and scour processes.

ACKNOWLEDGEMENTS

This work was supported by the three-year (2020-2023) research project NuLIMAS (Numerical Modelling of Wave-Induced Liquefaction Around Marine Structures) within the ERA-NET Co-fund MarTERA Program under EU Horizon 2020 Framework (Grant No. 728053), the German Federal Ministry for Economic Affairs and Climate Action (Grant No.03SX524A), the Scientific

and Technological Research Council of Turkey (Grant No. TEYDEB-1509/9190068), and the Polish National Centre for Research and Development (Grant MarTERA-2/NuLIMAS/3/2021).

REFERENCES

- Biot, M. (1941). General theory of three-dimensional consolidation. *Journal of applied physics*, pp. 155-164.
- De Alba, P., Chan, C., and Seed, H. (1976). Sand liquefaction in large-scale simple shear tests. *Journal of the Geotechnical Engineering Division*, pp. 909-927.
- Kazimierowicz-Frankowska, K., Kulczykowski, M., Majewski, D., and Smyczyński, M. (2023). Pore pressure generation in seabed under rocking-motion excitation. *submitted to the 33rd International Ocean and Polar Engineering Conference*. Ottawa, Canada.
- Kazimierowicz-Frankowska, K., Kulczykowski, M., Majewski, D., Mierczyński, J., and Smyczyński, M. (2022). The effect of the height of the regular wave on seabed liquefaction. *Proceedings of the ASME 2022 41st International Conference on Ocean, Offshore and Arctic Engineering*. Hamburg, Germany.
- Lemmer, F. (2018). *Low-Order Modeling, Controller Design and Optimization of Floating Offshore Wind Turbines*. PhD thesis, University of Stuttgart.
- NuLIMAS. (2020). *NuLIMAS project website*. <http://www.nulimas.info> [last access 20/02/2023]
- Shanmugasundaram, R. K., Rusche, H., Windt, C., Kirca, V.S.O., Sumer, B. M., and Goseberg, N. (2022). Towards the Numerical Modelling of Residual Seabed Liquefaction Using OpenFOAM. *OpenFOAM Journal*, pp. 94-115.
- Sumer, B. M. (2014). *Liquefaction Around Marine Structure*. World Scientific.
- Sumer, B. M., Hatipoglu, F., and Fredsøe, J. (2007). Wave scour around a pile in sand, medium dense, and dense silt. *Journal of waterway, port, coastal, and ocean engineering*, pp. 14-27.
- Sumer, B. M. and Kirca, V.S.O. (2021). Scour and liquefaction issues for anchors and other subsea structures in floating offshore wind farms: A review. *Water Science and Engineering*, pp. 3-14.
- Sumer, B. M., Özgür, V.S.O., and Fredsøe, J. (2012). Experimental validation of a mathematical model for seabed liquefaction under waves. *International Journal of Offshore and Polar Engineering*.
- Tonkin, S., Yeh, H., Kato, F., and Sato, S. (2003). Tsunami scour around a cylinder. *Journal of Fluid Mechanics*, pp. 165 - 192.
- Verruijt, A. (1969). Elastic storage of aquifers. *Flow through porous media*, pp. 331-376.
- Windt, C., Schimmels, S., Kudella, M., Shanmugasundaram, R., Rusche, H., Sumer, B. M., Kirca, V.S.O., Vanjakula, V., Adam, F., Majewski, D., Kazimierowicz-Frankowska, K., Hrycyna, G., Goseberg, N. (2022). Numerical modelling of liquefaction around marine structures – Progress and recent developments. *Proceedings of the ASME 41st International Conference on Ocean, Offshore and Arctic Engineering*. Hamburg, Germany.
- Windt, C., Shanmugasundaram, R., Schimmels, S., Kudella, M., Rusche, H., Kirca, V.S.O., Sumer, B.M., Vanjakula, V., Adam, F., Majewski, D., Kazimierowicz-Frankowska, K., Pietrzekiewicz, M., Goseberg, N. (2023). Numerical modelling of liquefaction around marine structures in the OpenFOAM framework. *submitted for the 10th European Conference on Numerical Methods in Geotechnical Engineering*. London, UK.